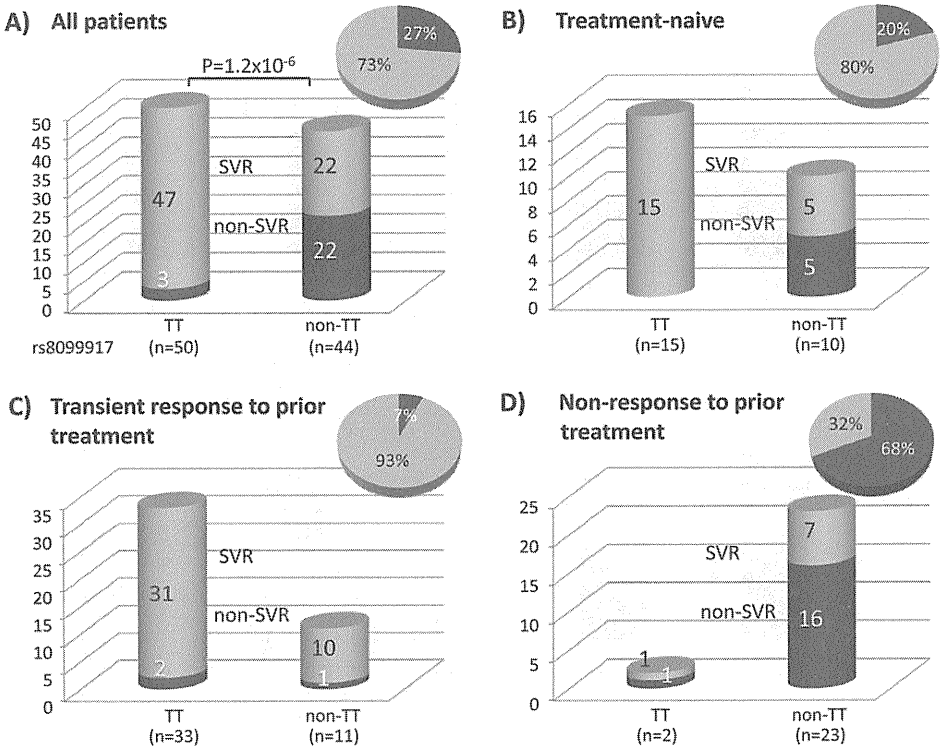

Figure 1. SVR frequency after triple therapy grouped by IL128B SNP rs8099917 genotype and by response to previous interferon (IFN) treatment. *A*, All patients. *B*, Treatment-naive patients. *C*, Previously treated patients who responded transiently to therapy. *D*, Previously treated patients who failed to respond to therapy. Inset pie charts indicate percentage of SVR *(light gray)* and non-SVR *(dark gray)* patients.

resulted in dose reduction according to the treatment protocol, no significant effects on SVR rate resulting from dose reduction were observed.

Viral Substitutions

The 43 patients (46%) with a substitution at position 70 of the HCV core protein (core70) were significantly less likely to achieve SVR than were patients with wild-type core70 (60% vs 86%; $P = .01$). There was no difference in SVR rate due to substitution at position 91 (core91; 81% vs 67%; $P = .17$) (Figure 2). There was also no difference in SVR rate due to substitutions in the NS5A ISDR region ($P = .43$). Patients with rs8099917 genotype TT were significantly more likely to be associated with wild-type core70 or core91 ($P = .006$ and $P = .031$, respectively). There was no association between rs809917 genotype and ISDR substitutions ($P = .94$).

Predictive Factors for RVR

RVR, defined as undetectable HCV RNA levels at week 4 of treatment, is a strong on-treatment predictor of SVR [34]. Previous IFN treatment, time to first ribavirin dose reduction, and baseline hemoglobin levels were each significant univariate predictors, but only hemoglobin level was a significant independent predictor of RVR under multiple logistic regression ($P = .028$; OR, 3.11).

Predictive Factors for SVR

Significant univariate predictors for SVR included clinical factors (γGTP level; rs8099917 genotype), viral factors (core70 substitutions), response to prior treatment (relapse or nonresponse), and on-treatment factors (RVR) (Table 3). Of these, nonresponse to prior treatment, rs8099917 genotype, RVR, and core70 substitutions were retained in the multivariate model, and nonresponse to prior treatment (OR, .17; $P = .01$), rs8099917 genotype (OR, .12; $P = .014$), and RVR (OR, 14.0; $P = .0064$) were identified as significant independent predictors for SVR. When only pretreatment factors were considered, nonresponse to prior treatment (OR, .14; $P = .0028$) and rs8099917 genotype (OR, .19; $P = .027$) were the only independent predictors.

DISCUSSION

This study showed that patients undergoing PEG-IFN, ribavirin, and telaprevir triple therapy for chronic hepatitis C genotype 1 infection achieve a higher SVR rate than typically expected under combination therapy alone in Japanese patients. Moreover, patients who showed transient response in previous treatment were more likely to achieve SVR after triple therapy, whereas nonresponders to prior treatment remained unlikely to eradicate the virus. Considering that telaprevir has a mode of

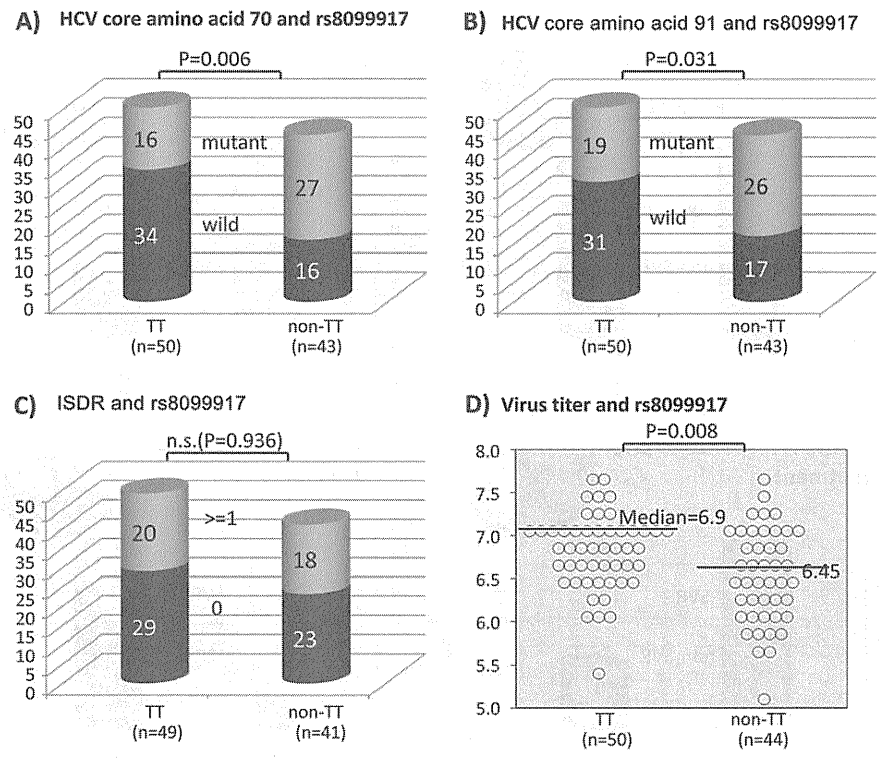

Figure 2. Viral factors and IL128B SNP rs8099917 genotype. *A*, Substitutions at HCV core amino acid 70. *B*, Substitutions at core amino acid 91. *C*, Frequency of patients with ≥2 substitutions in the NS5A interferon sensitivity determining region. *D*, Baseline viral load.

action different from that of IFN and ribavirin, [5] it is surprising that triple therapy does not better improve SVR rates among prior nonresponders, suggesting that additional unknown factors contribute to nonresponse. However, the duration of triple therapy, followed by standard of care, was limited to 24 weeks in this study; therefore, it is possible that prior nonresponders and patients who experienced relapse may benefit from a longer duration of therapy.

The most interesting result from this study is the high SVR rate among patients who previously experienced relapse, even

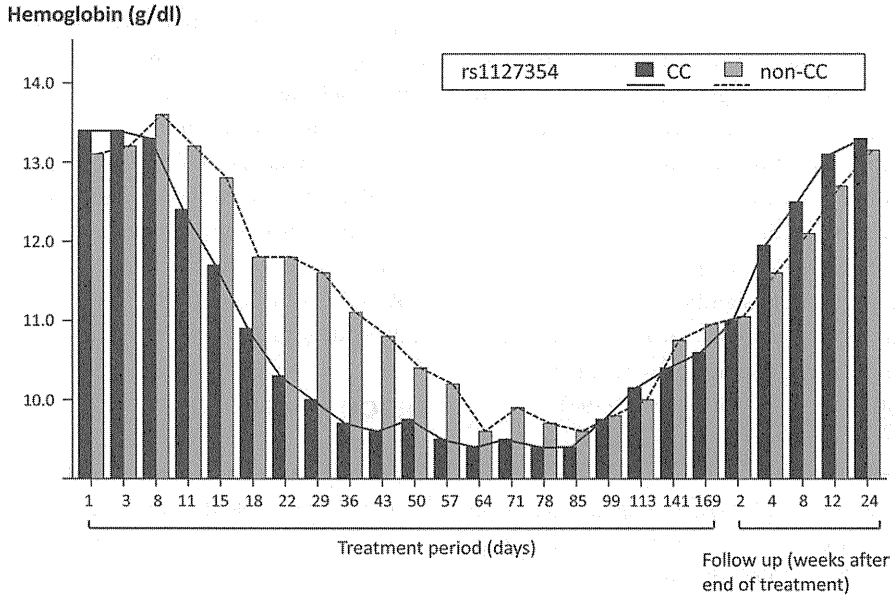

Figure 3. Change in hemoglobin level by ITPA SNP during triple therapy. Hemoglobin levels in patients grouped by ITPA SNP rs1127354 genotype (solid line represents CC; dashed line represents non-CC).

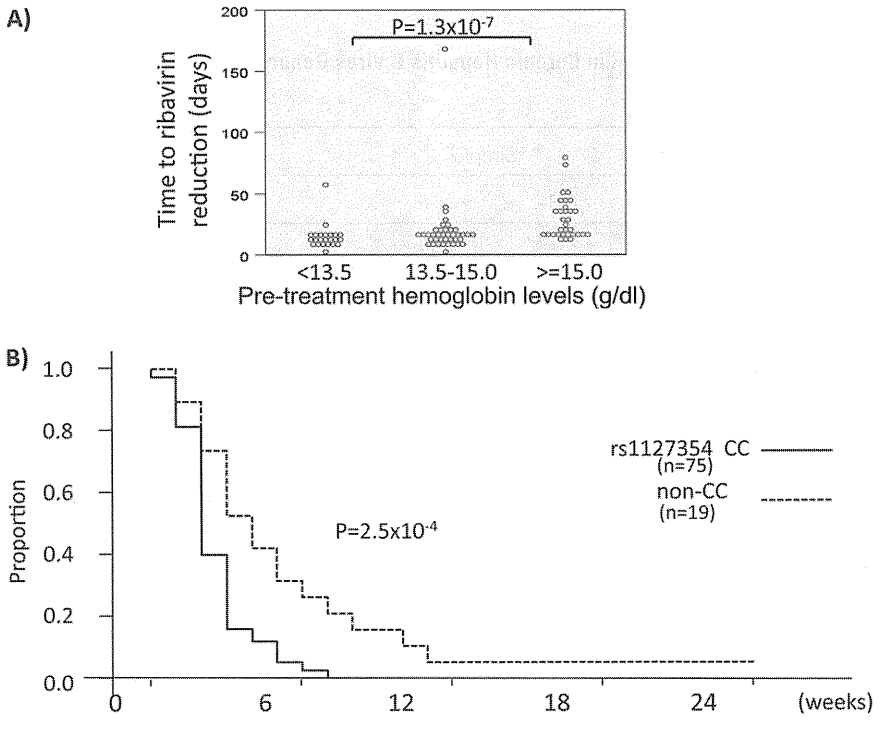

Figure 4. Ribavirin dose reduction during triple therapy. *A*, Number of days of treatment until first ribavirin dose reduction, by pretreatment hemoglobin levels. *B*, Kaplan-Meier curve for dose reduction grouped by ITPA SNP rs1127354 genotype (solid line represents CC; dashed line represents non-CC).

compared with that of naive patients. This is partly because of the higher frequency of the favorable rs8099917 TT genotype among patients who previously experienced relapse (33 [75%] of 44) than among naive patients (15 [60%] of 25), which perhaps reflects the fact that all patients who previously experienced relapse demonstrated at least a transient response to combination therapy and that this group is less likely to include as many patients with non-TT genotypes. All of the treatment-naive patients with the favorable genotype (15 [100%] of 15) achieved SVR, compared with 31 (94%) of 33 patients who previously experienced relapse; conversely, only one-half of the treatment-naive patients with unfavorable rs8099917 genotypes (5 [50%] of 10) achieved SVR, compared with only 1 (9%) of 11 of the patients who previously experienced relapse. This suggests that, although patients who previously experienced relapse have a demonstrated potential to respond to the therapy, there should be more variability among naive patients. Another consideration is that the frequency of the favorable wild-type core70 amino acid was slightly higher among patients who previously experienced relapse (28 [64%] of 44) than among naive patients (13 [52%] of 25). It should be noted, however, that the small number of patients in this study limits the conclusions that can be drawn, and results should be verified in a larger study, perhaps using stratified sampling based on patient background with regard to treatment history to establish more homogeneous patient populations.

In this and a number of other studies, variation in the IL28B locus remains the strongest predictor of SVR reported to date [16–18, 35]. It is unclear which, if any, of the reported SNPs is the primary or functional SNP, but most studies report results for rs8099917 and/or rs12979860, which are under strong linkage disequilibrium in Japanese patients and fall within the intergenic region upstream of IL28B. Although the mechanism is unknown, IL28B and the other 2 members of the IFN-λ family, IL28A and IL29, code for type III IFNs, which are similar to type I IFNs but use a highly tissue-specific receptor [36, 37]. IFN-stimulated genes appear to be initially down-regulated in patients with the favorable rs8099917 TT genotype [38], which may help to prevent desensitization and promote maximal induction of IFN-stimulated genes, although mechanistic studies are needed to understand the connection between IL28B and SVR.

In addition to IL28B polymorphisms, a number of studies have reported that amino acid substitutions in the HCV core protein and the ISDR region of NS5A independently predict treatment outcome after combination therapy [14, 22, 28, 30], and these findings have recently been extended to triple therapy[39, 40]. In this study, substitution at core70 was significant in univariate tests and was selected for inclusion in the multivariate model, but it was not significant in multiple logistic regression. One reason for this may be that core substitutions were initially reported to be associated with nonresponse [22], whereas this study focused on SVR because of the very small number of nonresponders. Terms that are significant in univariate but not multivariate tests may be correlated with each

Table 3. Predictive Factors Associated With SVR in Chronic Hepatitis C Virus Genotype 1 Patients Who Received Pegylated Interferon/Ribavirin/Telaprevir Triple Therapy

	Simple				Multiple			
Variable	*n*	OR	*P*		OR	(95% CI)	*P*	
Treatment-naive	94	1.6	.389					
Previous non-responder	94	0.1	5.5E-08	***	0.17	(.04–.66)	.010	*
Previous relapser	94	10.7	5.2E-05	***				
Age	94	0.8	.939					
Sex (male vs female)	94	1.5	.100					
BMI (kg/m2)	94	0.9	.558					
rs8099917 (TT vs GT/GG)	94	0.1	1.7E-06	***	0.12	(.02–.65)	.014	*
rs1127354 (CC vs AC/AA)	94	1.0	.980					
Core aa70 (wt vs mutant)	93	0.2	.0053	**	0.35	(.09–1.31)	.119	
Core aa91 (wt vs mutant)	93	0.5	.111					
ISDR (0–1 vs ≥2)	90	1.7	.308					
Viral load	94	1.1	.560					
ALT (IU/L)	94	0.9	.142					
gammaGTP	94	0.7	.0009	***				
Hemoglobin (g/dL)	94	1.4	.292					
WBC (/mm^3)	94	1.3	.271					
Platelets (×104/mm^3)	94	1.7	.165					
Total cholesterol (mg/dL)	94	1.7	.160					
LDL cholesterol (mg/dL)	94	2.6	.018	*				
Days to first ribavirin dose reduction	94	1.2	.129					
RVR	94	10.8	4.4E-05	***	14.00	(2.10–93.2)	.006	**
EVR	94	7992.0	.004	**				

NOTE. Results of simple and multiple logistic regression are shown. The multivariate model was constructed using stepwise selection of univariate terms significant at the .05 level. Symbols: * ($P < .05$), ** ($P < .01$), *** ($P < .001$).

other, and only the factor with the strongest effect remains significant. In this case, core70 is significantly correlated with the stronger rs8099917 genotype ($r = .31$; $P = .0027$), although other studies have shown that these terms contribute independently, especially when a larger number of patients are included [39]. Without knowing the mechanism underlying either factor, it is not possible to determine whether the underlying factors that they represent are in fact independent or whether they represent different aspects of a common unknown factor.

Although novel therapies that are not based on IFN and ribavirin are urgently needed, the pending introduction of protease inhibitors represents a pivotal addition to the treatment arsenal, especially for patients who show at least partial response to combination therapy. Because telaprevir is effective as monotherapy, even if only briefly until resistant mutations emerge, alternate combination therapies based on telaprevir and another component designed to raise the barrier to resistance may provide an adequate alternative for older patients and patients unable to tolerate IFN or ribavirin. Furthermore, identification of additional SNPs associated with anemia and other adverse effects will help reduce complications and the need for dose reductions and may lead to treatment guidelines for at-risk patients, such as administration of erythropoietin to stimulate erythropoiesis [41]. Ribavirin dose reductions were required significantly earlier in patients with ITPA SNP genotype CC, compared with patients with non-CC genotypes, which may contribute to poorer response if cumulative ribavirin administration decreases to <80% of the planned dose [26], although ribavirin dose reduction did not affect SVR rate in this study.

In conclusion, triple therapy with PEG-IFN, ribavirin, and telaprevir resulted in higher rates of SVR, compared with PEG-IFN plus ribavirin combination therapy, especially among treatment-naive patients and patients who showed transient response to prior treatment. ITPA polymorphisms predict ribavirin-induced anemia but are not associated with SVR, whereas IL28B polymorphisms and early viral kinetics remain the strongest predictors of SVR with use of triple therapy. Considering both host and viral factors, we identified 2 subgroups of patients who responded well to triple therapy: patients with the favorable rs8099917 TT genotype (47 [94%] of 50) and patients with non-TT genotypes who had wild-type core70 and core91 amino acids (7 [78%] of 9). Patients matching these conditions would benefit most from this 24-week triple therapy, whereas a longer duration of therapy should perhaps be considered for the remaining difficult-to-treat patients.

Funding

This work was supported by Grants-in-Aid for scientific research and development from the Ministry of Health, Labor and Welfare, Government of Japan.

Acknowledgments

We thank Mika Tsuzuno, Sakura Akamatsu, Sanae Furuya, and other members of the clerical and medical staff at Hiroshima University Hospital for their help.

References

1. Alter MJ. Epidemiology of hepatitis C in the West. Semin Liver Dis **1995**; 15:5–14.
2. Shepard CW, Finelli L, Alter MJ. Global epidemiology of hepatitis C virus infection. Lancet Infect Dis **2005**; 5:558–67.
3. Chevaliez S, Pawlotsky JM. Hepatitis C virus: virology, diagnosis and management of antiviral therapy. World J Gastroenterol **2007**; 13:2461–6.
4. Hadziyannis SJ, Sette H Jr, Morgan TR, et al. Peginterferon-alpha2a and ribavirin combination therapy in chronic hepatitis C: a randomized study of treatment duration and ribavirin dose. Ann Intern Med **2004**; 140:346–55.
5. Jang JY, Chung RT. New treatments for chronic hepatitis C. Korean J Hepatol **2010**; 16:263–77.
6. Fowell AJ, Nash KL. Telaprevir: a new hope in the treatment of chronic hepatitis C. Adv Ther **2010**; 27:512–22.
7. Foy E, Li K, Wang C, et al. Regulation of interferon regulatory factor-3 by the hepatitis C virus serine protease. Science **2003**; 300:1145–8.
8. Reesink HW, Zeuzem S, Weegink CJ, et al. Rapid decline of viral RNA in hepatitis C patients treated with VX-950: a phase Ib, placebo-controlled, randomized study. Gastroenterology **2006**; 131:997–1002.
9. Sarrazin C, Kieffer TL, Bartels D, et al. Dynamic hepatitis C virus genotypic and phenotypic changes in patients treated with the protease inhibitor telaprevir. Gastroenterology **2007**; 132:1767–7.
10. McHutchison JG, Everson GT, Gordon SC, et al. Telaprevir with peginterferon and ribavirin for chronic HCV genotype 1 infection. N Engl J Med **2009**; 360:1827–38.
11. McHutchison JG, Manns MP, Muir AJ, et al. Telaprevir for previously treated chronic HCV infection. N Engl J Med **2010**; 362:1292–303.
12. Suzuki F, Suzuki Y, Akuta N, et al. Sustained virological response in a patient with chronic hepatitis C treated by monotherapy with the NS3-4A protease inhibitor telaprevir. J Clin Virol **2010**; 47:76–8.
13. Dienstag JL, McHutchison JG. American Gastroenterological Association technical review on the management of hepatitis C. Gastroenterology **2006**; 130:231–64; quiz 214–7.
14. Akuta N, Suzuki F, Kawamura Y, et al. Predictive factors of early and sustained responses to peginterferon plus ribavirin combination therapy in Japanese patients infected with hepatitis C virus genotype 1b: amino acid substitutions in the core region and low-density lipoprotein cholesterol levels. J Hepatol **2007**; 46:403–10.
15. Romero-Gómez M, Del Mar Viloria M, Andrade R, et al. Insulin resistance impairs sustained response rate to peginterferon plus ribavirin in chronic hepatitis C patients. Gastroenterology **2005**; 128:636–41.
16. Ge DL, Fellay J, Thompson AJ, et al. Genetic variation in IL28B predicts hepatitis C treatment-induced viral clearance. Nature **2009**; 461:399–401.
17. Tanaka Y, Nishida N, Sugiyama M, et al. Genome-wide association of IL28B with response to pegylated interferon-alpha and ribavirin therapy for chronic hepatitis C. Nat Genet **2009**; 41:1105–9.
18. Suppiah V, Moldovan M, Ahlenstiel G, et al. IL28B is associated with response to chronic hepatitis C interferon-alpha and ribavirin therapy. Nat Genet **2009**; 41:1100–U74.
19. Thomas DL, Thio CL, Martin MP, et al. Genetic variation in IL28B and spontaneous clearance of hepatitis C virus. Nature **2009**; 461:798–801.
20. Zeuzem S, Franke A, Lee JH, Herrmann G, Ruster B, Roth WK. Phylogenetic analysis of hepatitis C virus isolates and their correlation to viremia, liver function tests, and histology. Hepatology **1996**; 24:1003–9.
21. Enomoto N, Sakuma I, Asahina Y, et al. Comparison of full-length sequences of interferon-sensitive and resistant hepatitis-C virus 1b—sensitivity to interferon is conferred by amino-acid substitutions in the NS5A region. J Clin Invest **1995**; 96:224–30.
22. Akuta N, Suzuki F, Sezaki H, et al. Association of amino acid substitution pattern in core protein of hepatitis C virus genotype 1b high viral load and non-virological response to interferon-ribavirin combination therapy. Intervirology **2005**; 48:372–80.
23. Fellay J, Thompson A, Ge D, et al. ITPA gene variants protect against anaemia in patients treated for chronic hepatitis C. Nature **2010**; 464:405–8.
24. Thompson A, Fellay J, Patel K, et al. Variants in the ITPA gene protect against ribavirin-induced hemolytic anemia and decrease the need for ribavirin dose reduction. Gastroenterology **2010**; 139:1181–9.
25. Ochi H, Maekawa T, Abe H, et al. ITPA polymorphism affects ribavirin-induced anemia and outcomes of therapy—a genome-wide study of Japanese HCV virus patients. Gastroenterology **2010**; 139:1190–7. e3.
26. McHutchison J, Manns M, Patel K, et al. Adherence to combination therapy enhances sustained response in genotype-1-infected patients with chronic hepatitis C. Gastroenterology **2002**; 123:1061–9.
27. Kumada H, Okanoue T, Onji M, et al. Guidelines for the treatment of chronic hepatitis and cirrhosis due to hepatitis C virus infection for the fiscal year 2008 in Japan. Hepatol Res **2010**; 40:8–13.
28. Akuta N, Suzuki F, Sezaki H, et al. Predictive factors of virological non-response to interferon-ribavirin combination therapy for patients infected with hepatitis C virus of genotype 1b and high viral load. J Med Virol **2006**; 78:83–90.
29. Desmet VJ, Gerber M, Hoofnagle JH, Manns M, Scheuer PJ. Classification of chronic hepatitis–diagnosis, grading and staging. Hepatology **1994**; 19:1513–20.
30. Enomoto N, Sakuma I, Asahina Y, et al. Mutations in the nonstructural protein 5A gene and response to interferon in patients with chronic hepatitis C virus 1b infection. New Engl J Med **1996**; 334:77–81.
31. Rauch A, Kutalik Z, Descombes P, et al. Genetic variation in IL28B is associated with chronic hepatitis C and treatment failure: a genome-wide association study. Gastroenterology **2010**; 138:1338–45, 1345 e1–7.
32. Ohnishi Y, Tanaka T, Ozaki K, Yamada R, Suzuki H, Nakamura Y. A high-throughput SNP typing system for genome-wide association studies. J Hum Genet **2001**; 46:471–7.
33. Suzuki A, Yamada R, Chang X, et al. Functional haplotypes of PADI4, encoding citrullinating enzyme peptidylarginine deiminase 4, are associated with rheumatoid arthritis. Nat Genet **2003**; 34:395–402.
34. Poordad F, Reddy KR, Martin P. Rapid virologic response: a new milestone in the management of chronic hepatitis C. Clin Infect Dis **2008**; 46:78–84.
35. Thompson AJ, Muir AJ, Sulkowski MS, et al. IL28B polymorphism improves viral kinetics and is the strongest pre-treatment predictor of SVR in HCV-1 patients. Gastroenterology **2010**; 139:120–9.e18.
36. Marcello T, Grakoui A, Barba-Spaeth G, et al. Interferons alpha and lambda inhibit hepatitis C virus replication with distinct signal transduction and gene regulation kinetics. Gastroenterology **2006**; 131:1887–98.
37. Kotenko SV, Gallagher G, Baurin VV, et al. IFN-lambdas mediate antiviral protection through a distinct class II cytokine receptor complex. Nat Immunol **2003**; 4:69–77.

38. Honda M, Sakai A, Yamashita T, et al. Hepatic ISG expression is associated with genetic variation in IL28B and the outcome of IFN therapy for chronic hepatitis C. Gastroenterology **2010**; 139:499–509.
39. Akuta N, Suzuki F, Hirakawa M, et al. Amino acid substitution in hepatitis C virus core region and genetic variation near the interleukin 28B gene predict viral response to telaprevir with peginterferon and ribavirin. Hepatology **2010**; 52:421–9.
40. Akuta N, Suzuki F, Hirakawa M, et al. Amino acid substitutions in the hepatitis C virus core region of genotype 1b affect very early viral dynamics during treatment with telaprevir, peginterferon, and ribavirin. J Med Virol **2010**; 82:575–82.
41. Dieterich D, Wasserman R, Bräu N, et al. Once-weekly epoetin alfa improves anemia and facilitates maintenance of ribavirin dosing in hepatitis C virus-infected patients receiving ribavirin plus interferon alfa. Am J Gastroenterol **2003**; 98:2491–9.

jraas

Journal of the Renin-Angiotensin-Aldosterone System
12(4) 462–468

DOI: 10.1177/1470320311415887
jra.sagepub.com
SAGE

Liver lipid content is reduced in rat given 7-day administration of angiotensin II

Nobukazu Ishizaka[1,2], Makiko Hongo[1], Aiko Sakamoto[1], Kan Saito[1], Kyoko Furuta[1] and Kazuhiko Koike[3]

Abstract

Activation of the renin–angiotensin system may be involved in the development of hepatic steatosis, a condition that is associated with insulin resistance. We showed that in rats, angiotensin II induced accumulation of triglycerides in the renal tubular and cardiac cells, although it significantly reduced the weight of the rats. Here we investigated the liver lipid content of rats given long-term angiotensin II administration. Angiotensin II (0.7 mg/kg/day) was infused into the rats for 7 days via an osmotic minipump. Some rats also received hydralazine or losartan concomitantly. It was shown that angiotensin II reduced oil red O-stainable lipid droplets (6% of the control value) and liver triglyceride content (angiotensin II: 4.6 ± 0.8 μg/mg, control: 11.7 ± 1.1 μg/mg). Both of these phenomena were blocked by losartan, but not by hydralazine. Angiotensin II infusion reduced the expression and activity of AMP-activated protein kinase. In addition, angiotensin II decreased the mRNA expression of peroxisome proliferator-activated receptor-α and genes related to β-oxidation, although mRNA expression of genes related to lipogenesis were not affected. Angiotensin II reduced triglyceride content in the liver, unlike in the kidney or heart, via an AT1 receptor-dependent mechanism.

Keywords

Angiotensin II, catecholamines, gene expression, hypertension, lipid accumulation

Introduction

It has been shown in previous studies that administration of angiotensin II in conjunction with bile duct ligation[1] exacerbated liver fibrosis, whereas blockade of the renin–angiotensin system (RAS), on the other hand, inhibited liver fibrosis and downregulated profibrotic genes expression in animals susceptible to liver fibrosis.[2-4] We showed that long-term administration of angiotensin II into rats upregulated expression of profibrotic genes in the liver, which might be in part related to the enhanced oxidative stress induced by this peptide.[5] Recent studies have shown that a certain proportion of non-alcoholic fatty liver disease (NAFLD) can progress to hepatic fibrosis (cirrhosis) and liver failure,[6] and the extent of hepatic steatosis is associated with fibrosis in chronic hepatitis C[7] and NAFLD.[8] In addition, AT_1 receptor blockade has an anti-fibrotic effect in the liver.[9,10] These studies suggest the possible role of excessive lipids accumulated in the liver in the development and promotion of liver fibrosis. It should be noted, however, that under certain conditions, accumulation of neutral lipids may prevent progressive liver damage in hepatic steatosis.[11]

In the previous experiments, we found that angiotensin II induced accumulation of lipids in the renal tubular epithelial[12] and cardiac cells,[13] where increased superoxide was produced and fibroproliferative gene expression were upregulated.[14] These changes were found to be suppressed by the AT_1 receptor blockade, suggesting the crucial role of angiotensin II–AT_1 receptor axis in the lipid accumulation in these tissues. These observations collectively lead us to investigate in the current study whether administration of angiotensin II increases lipid content in the liver, as has been observed in the kidney and heart.

Materials and methods

Animal models

The experiments were performed in accordance with the guidelines for animal experimentation approved by the

[1] Department of Cardiovascular Medicine, University of Tokyo Graduate School of Medicine, Tokyo, Japan
[2] Department of Internal Medicine III, Division of Cardiology, Osaka Medical College, Faculty of Medicine, Osaka, Japan
[3] Department Infectious Diseases, University of Tokyo Graduate School of Medicine, Tokyo, Japan

Corresponding author:
Nobukazu Ishizaka, Department of Internal Medicine III, Division of Cardiology, Osaka Medical College, Faculty of Medicine, Takatsuki-shi Daigaku-machi 2-7, Osaka 569-8686, Japan.
Email: ishizaka@poh.osaka-med.ac.jp

Animal Center for Biomedical Research, Faculty of Medicine, University of Tokyo. Male Sprague–Dawley rats at 10 weeks of age were fed standard rat chow ad libitum. Angiotensin II-induced hypertension was induced in rats by subcutaneous implantation of an osmotic minipump (Alza Pharmaceutical) as described previously.[15] Briefly, Val^5-angiotensin II (Sigma Chemical) was infused at doses of 0.7 mg/kg/day. In some angiotensin II-infused rats, AT_1 receptor antagonist, losartan (25 mg/kg/day), or the nonspecific vasodilator, hydralazine (15 mg/kg/day) (Sigma Chemical), both of which normalized the blood pressure of angiotensin II-infused rats, was given in the drinking water.[16] Infusion of norepinephrine at a dose of 2.8 mg/kg/day for 7 days elevated blood pressure comparable to angiotensin II. Systolic blood pressure and heart rate were measured in conscious rats by tail-cuff plethysmography (BP-98A, Softron, Tokyo, Japan). Rats were sacrificed after overnight fasting in the metabolic cage.

Measurement of lipid content in the serum and the liver

Blood samples were taken just before the animals were killed. Serum levels of triglycerides (TG), total cholesterol (TG), and non-esterified fatty acid (NEFA) were measured by enzymatic methods (SRL). Liver contents triglycerides and total cholesterol were measured from homogenate extracts by enzymatic colorimetric determination using Triglyceride-E Test, Cholesterol-E Test, and Free cholesterol-E Test Wako, respectively (Wako Pure Chemicals).

Histological analysis

Oil red O staining was performed on sections of unfixed, freshly frozen heart samples (3 μm in thickness). The areas of lipid deposition were calculated by using the image analysis software, Photoshop (Adobe), and semiquantification of the lipid deposition was performed as described previously.[14]

Western blot analysis

Western blot analysis was performed as described previously.[17] Polyclonal antibodies against AMP-activated protein kinase α (AMPKα), and phospho-AMPKα (Thr172) (Cell Signaling) were used at a dilution of 1/1000.

Real-time reverse transcription polymerase chain reaction

Expression of lipid metabolism-related gene mRNA was analyzed by real-time quantitative polymerase chain reaction (PCR) performed by LightCycler together with hybriprobe technology (Roche Diagnostics). Expression of target genes was normalized to the mRNA expression of endogenous control, glyceraldehyde-3-phosphate dehydrogenase (GAPDH). The target genes were as follows: peroxisome proliferator-activated receptor (PPAR)-α (Nihon Gene Research Lab's Inc., Sendai, Japan), sterol regulatory element-binding protein (SREBP)-1c, fatty acid synthase (FAS), 3-hydroxy-3-methylglutaryl coenzyme A reductase (HMG-CoAR), carnitine palmitoyltransferase (CPT)-1, PPAR-γ coactivator (PGC)-1α, and uncoupling protein (UCP)2. The forward and backward primers used are described in Supplementary Table 1.

Statistical analysis

Data are expressed as the mean ± the standard error of the mean (SEM). We used analysis of variance (ANOVA) followed by a multiple comparison test to compare raw data, before expressing the results as a percentage of the control value using the statistical analysis software StatView version 5.0 (SAS Institute). A value of $p < 0.05$ was considered to be statistically significant.

Results

Characteristics of experimental rats

Administration of angiotensin II caused an increase in the blood pressure, which was blocked by either hydralazine or losartan (Supplementary Table 2). Losartan, but not hydralazine, suppressed the increase in serum levels of TC, TG and NEFA, induced by angiotensin II. At 7 days of infusion, angiotensin II had decreased the body weight (255 ± 5 g [$n = 6$], $p < 0.0001$ versus control) compared with untreated controls (323 ± 12 g [$n = 8$]); this decrease was suppressed by losartan (316 ± 4 [$n = 5$], p = NS versus control), but not by hydralazine (231 ± 10 g [$n = 5$], $p < 0.0001$ versus control). Norepinephrine infusion did not affect body weight (300±17 [n=4] NS versus control) as compared with untreated controls

Staining for lipids

Oil red O staining of liver sections showed that lipid droplets were present in hepatocytes in the untreated controls (Figure 1). In contrast, the extent of oil red O-positive lipid droplets was decreased after angiotensin II infusion, and this decrease was inhibited by losartan, but not by hydralazine (Figure 1(C)–(H)). This finding contrasts with the increased accumulation of lipid droplets in the kidney (Figure 1(I) and (J)) and heart (Figure 1(K) and (L)) of angiotensin II-infused rats observed in detail in previous studies.[12,18] Norepinephrine infusion did not significantly alter lipid deposition (98 ± 4% of control [$n = 4$], p = NS versus control).

Tissue content of lipids

The tissue content of TG, TC, and free cholesterol was found to be reduced in the liver of angiotensin II-infused

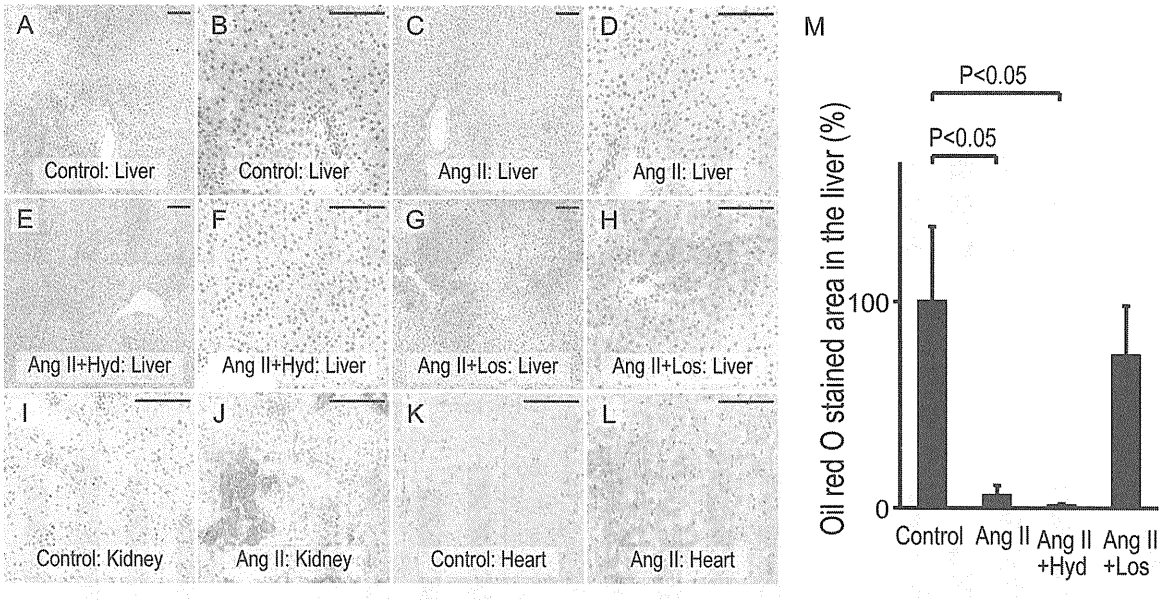

Figure 1. Oil red O staining of the liver of rats given angiotensin II with or without depressor agents. (A), (B) Liver section from an untreated control rat. (C), (D) Liver sections from an angiotensin II (Ang II)-infused rat. (E), (F) Liver sections from rat given both Ang II and hydralazine (Hyd). (G), (H) Liver section from a rat given both Ang II and losartan (Los). (I) Kidney section from an untreated control rat. (J) Kidney section from an Ang II-infused rat. (K) Heart section from an untreated control rat. (L) Heart section from Ang II-infused rat. Lipid droplets were present in the liver of control rats (A, B). Ang II infusion decreased the lipid droplets in the liver (C, D); this decrease was not suppressed by hydralazine (E, F), but was suppressed by losartan (G, H). As has been shown before, Ang II treatment induced an accumulation of lipids in the kidney (I, J) and in the heart (K, L). Original magnification, ×200. Scale bar, 100 μm. M. Semiquantification of the oil red O-stained area. Summary of data from four to five experiments in each group.

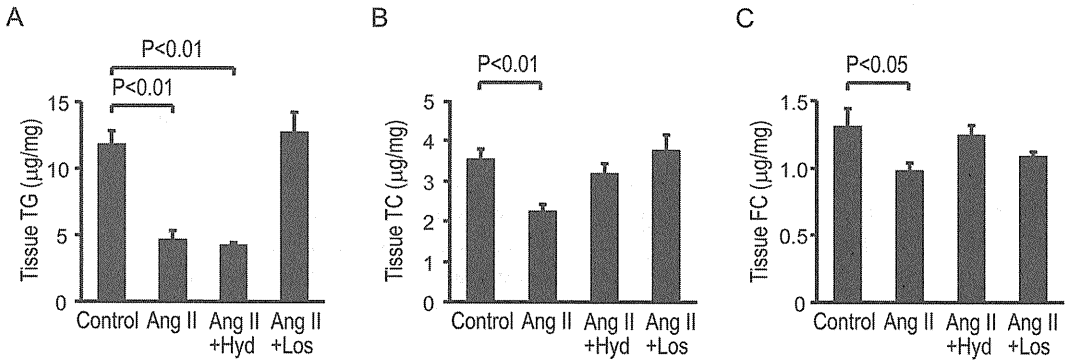

Figure 2. Tissue content of lipids. Content of (A) triglycerides (TG), (B) total cholesterol (TC) and (C) free cholesterol (FC) in the liver. Shown is a summary of data from five to seven rats in each group. Ang II, angiotensin II; Hyd, hydralazine; and Los, losartan.

rats (Figure 2). Hydralazine suppressed the angiotensin II-induced reduction in hepatic TC and free cholesterol content, but not TG content. Losartan reversed the angiotensin II-induced reduction in all three lipid fractions tested. On the other hand, Norepinephrine infusion did not significantly alter the hepatic TG content (11.7 ± 2.1 μg/mg [n = 7], p = NS versus control).

Regulation of genes related to lipid metabolism

We then examined the expression of lipid metabolism-related genes in the liver. The mRNA expression of genes related to lipid synthesis (SREBP-1c, FAS, and HMG-CoAR) was not found to be significantly changed in the liver of angiotensin II-infused rats (Figure 3). The

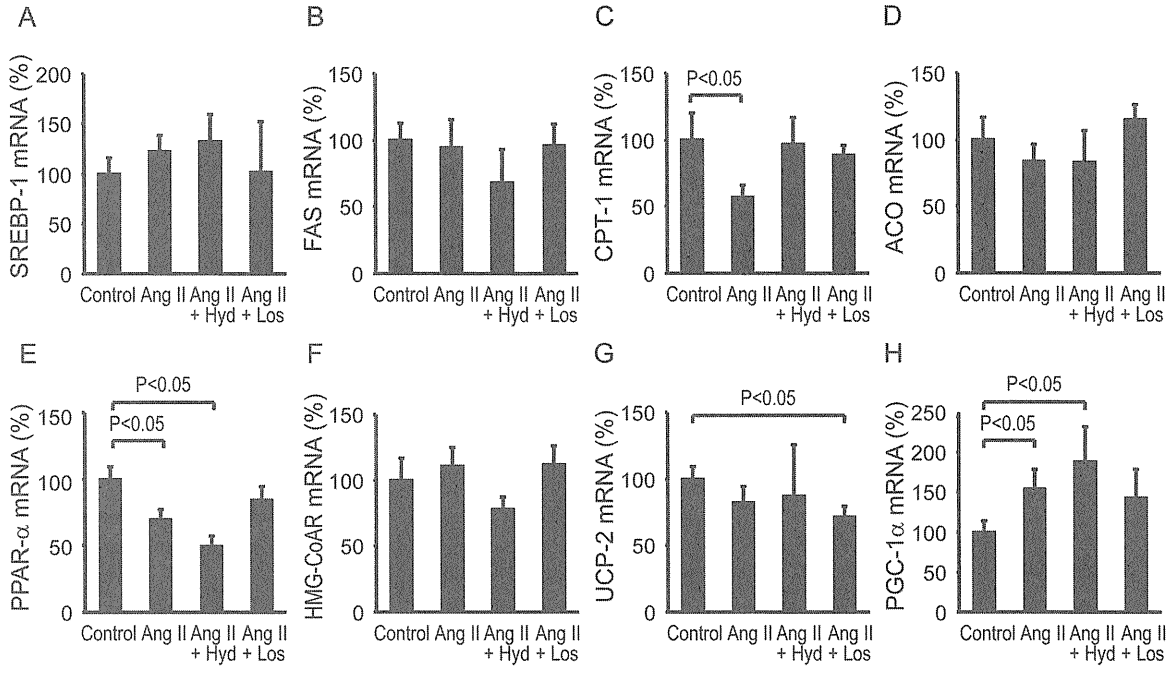

Figure 3. mRNA levels of genes related to lipid metabolism. Shown is a summary of data from five or six rats in each group. Ang II, angiotensin II; Hyd, hydralazine; and Los, losartan.

expression of PGC-1α was increased by angiotensin II, and this increase was suppressed by losartan, but not by hydralazine. PPAR-α mRNA expression was found to be downregulated by angiotensin II, and expression of CPT-1, a downstream target of PPAR-α, was also downregulated by angiotensin II, although the expression of ACO and UCP2 was not significantly changed by angiotensin II. The protein expression and activity of AMP-activated protein kinase (AMPK) was reduced by angiotensin II infusion, and this reduction was suppressed completely by losartan, and partially by hydralazine (Figure 4).

Discussion

In the current study, we showed that 7-day administration of angiotensin II decreased the content of TG, TC and free cholesterol in the liver. This angiotensin II-induced decrease in liver TG was suppressed by losartan, but not by hydralazine, indicating that it was an AT1-recepor-dependent and pressor-independent phenomenon. The mRNA expression of genes related to β-oxidation was downregulated (CPT-1, PPAR-α) or unchanged (ACO, UCP2) and those related to lipogenesis (SREBP-1, FAS, HMG-CoAR) was unchanged in the liver by angiotensin II infusion. These findings were in contrast to our previous findings that accumulation of TG occurred in the kidney and heart of the same animal model,[12,13] indicating that angiotensin II-induced lipid accumulation is somehow tissue-specific, which is different from the case of diabetes in which accumulation of excessive lipids can be seen in the liver[19] as well as the kidney[20] and heart,[21] and accompanied by a modulation of lipid metabolism-related genes in these tissues.[20, 22-23] We also found that oil red O-stainable lipid was increased in the liver (unpublished observations) as well as in the kidney and heart of the rat model of metabolic syndrome.[24]

That angiotensin II reduced liver lipid content in the liver was rather unexpected in the current study. Although we did not look into the detailed mechanism underlying the decrease in liver lipids by angiotensin II, there may be several possible explanations. The expression of lipogenic genes SREBP-1 and FAS was increased in the kidney and the heart of angiotensin II-infused rats;[14, 18] in the liver, by contrast, mRNA expression of these lipogenic genes was not significantly altered by angiotensin II infusion. In addition, mRNA expression of CPT-1, a mitochondrial β-oxidation enzyme, and the protein expression and activity of AMPK, a molecule that is implicated in the regulation of lipid oxidation are changes that would presumably act to increase liver lipid content.[25,26] Therefore, the reduction in hepatic lipid content caused by angiotensin II may not be a direct consequence of the angiotensin II-induced regulation of lipid metabolism-related gene expression.

A recent study showed that caloric restriction, which would induce lipolysis and subsequent mobilization of fat from storage,[27] increased TG content in the heart, but

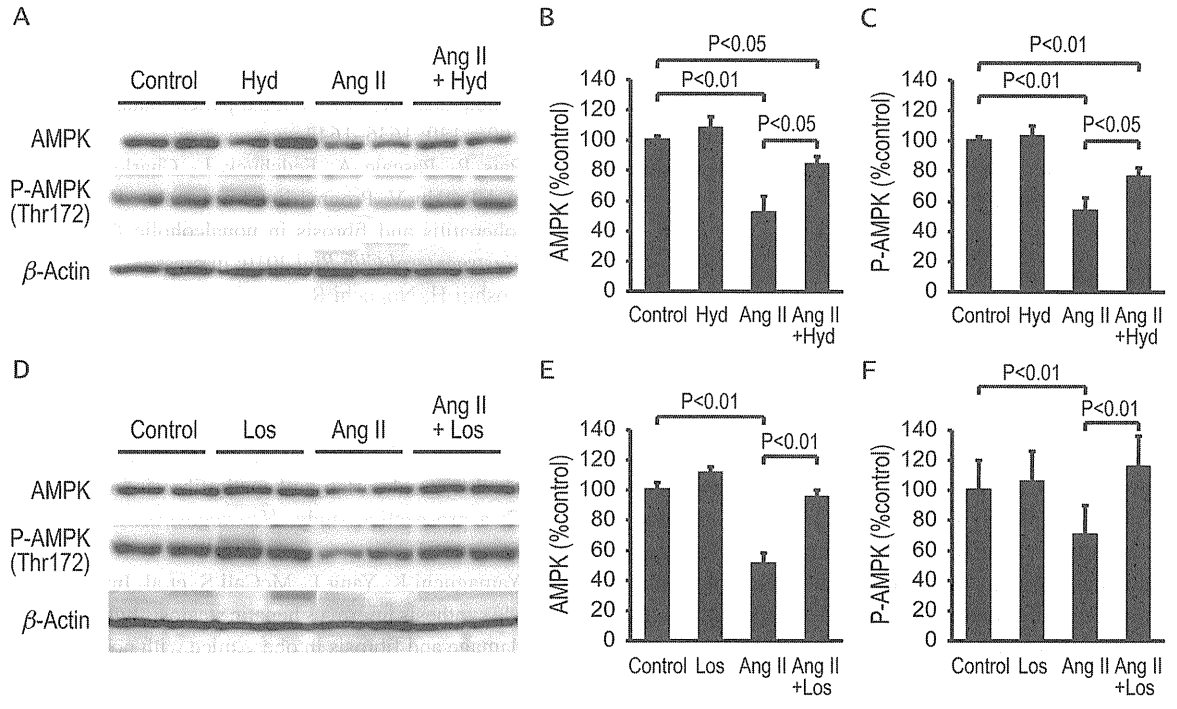

Figure 4. Western blot analysis of AMP-activated protein kinase α (AMPK), and the phosphorylated (activated) form of AMPKα (P-AMPK). (A), (D) Representative blots. (B), (C), (E), (F) Summary of data from four to six experiments in each group. Ang II, angiotensin II; Hyd, hydralazine; and Los, losartan.

deceased it in the liver.[28,29] It has been shown that angiotensin II infusion causes weight loss by enhancing catabolism.[30-32] In addition, a pressor dose of angiotensin II exerts lipolytic properties on both subcutaneous and visceral adipose tissue.[33] Therefore, it is possible that administered angiotensin II may have enhanced the lipolysis resulting in a re-distribution of tissue lipids, a scenario similar to that in caloric restriction. It is suggested that lipolysis induced by angiotensin II is in part by activation sympathetic tone and stimulation of the β-adrenergic-receptor,[33] events that may also occur during caloric restriction.[34] On the other hand, however, stimulation of the β-adrenergic receptor by the administration of norepinephrine did not alter hepatic lipid content, although it increased blood pressure to a comparable level to angiotensin II. Another possibility is that reduction of liver fat content by angiotensin II infusion might be attributed to increased the hepatic catabolism via activating IGF-1 signaling, a scenario that is suggested in the skeletal muscle.[35,36]

It is possible that the dosage of angiotensin II we used may be too high; however; our previous study showed that the plasma angiotensin II concentration was about three times higher in angiotensin II-infused rats compared with non-treated rats.[37]

Our results do not immediately indicate that activation of RAS will suppress the development of hepatic steatosis. It was shown that blockade of the AT_1 receptor suppressed the development of hepatic steatosis[38-40] in hepatic steatosis-prone animal models, and that long-term administration of angiotensin II to rats at a lower dose (0.14 mg/kg/day), which did not result in the loss of weight, induced hepatic steatosis.[41,42] In addition, in the transgenic rat that harbors mouse renin gene, a rat model of increased RAS activity, progressive hepatic steatosis was shown, and reduced β-oxidation, but not upregulation of genes involved in fatty acid synthesis could be observed.[43,44] Interestingly, body weight was not found to be decreased in these transgenic mice compared with wild-type controls.

In a preliminary study, we found that AT_1 blockade reduced the liver lipid content in the Otsuka Long–Evans Tokushima Fatty (OLETF) rat, a rat model of metabolic syndrome, and that AT_1 receptor blockage increased the activity of AMPK in the liver of this rat model of metabolic syndrome, opposite direction against that observed in the current study (Supplementary Figure). Furthermore, other groups' experiments showed that AT_1 receptor blockage improved insulin sensitivity in insulin-resistant rat,[45] whereas infusion of angiotensin II decreased insulin sensitivity in rats.[46] These findings may support the notion that a substantial difference exists in the role of activation of angiotensin II–AT_1 receptor axis between angiotensin II-infused hypertension animal model and non-infused

animal model with certain metabolic abnormalities. These discrepancies may be caused by the difference in the levels of circulating angiotensin II and systemic blood pressure, and the hypoperfusion of muscular tissue by angiotensin II-induced vascular constriction. These possibilities should be investigated in future studies.

Conclusions

In the liver, unlike in the kidney and heart, long-term administration of a pressor dose of angiotensin II caused a reduction of hepatic TG content by an AT1 receptor-dependent mechanism. The mRNA expression of some β-oxidation-related genes (CPT-1, PPAR-α) was downregulated where as that of some lipogenesis-related genes (SREBP-1, FAS, HMG-CoAR) was unchanged in the liver by angiotensin II infusion. These findings suggest that angiotensin II infusion decreases hepatic lipid content, which may not be medicated by the modulation gene expression related to lipogenesis and β-oxidation.

Acknowledgement

We are highly appreciative of Naoko Amitani for their excellent technical assistance.

Funding

This work was supported by the Ministry of Education, Science, and Culture of Japan Grant in Aid for Scientific Research (grant number 19590937), the Novartis Foundation for Gerontological Research, the Takeda Science Foundation, the Sankyo Foundation of Life Science, and Okinaka Memorial Institute for Medical Research.

References

1. Bataller R, Gabele E, Parsons CJ, et al. Systemic infusion of angiotensin II exacerbates liver fibrosis in bile duct-ligated rats. *Hepatology* 2005; 41: 1046–1055.
2. Paizis G, Gilbert RE, Cooper ME, et al. Effect of angiotensin II type 1 receptor blockade on experimental hepatic fibrogenesis. *J Hepatol* 2001; 35: 376–385.
3. Tox U and Steffen HM. Impact of inhibitors of the renin–angiotensin–aldosterone system on liver fibrosis and portal hypertension. *Curr Med Chem* 2006; 13: 3649–3661.
4. Hirose A, Ono M, Saibara T, et al. Angiotensin II type 1 receptor blocker inhibits fibrosis in rat nonalcoholic steatohepatitis. *Hepatology* 2007; 45: 1375–1381.
5. Ishizaka N, Saito K, Noiri E, et al. Administration of ANG II induces iron deposition and upregulation of TGF-beta1 mRNA in the rat liver. *Am J Physiol Regul Integr Comp Physiol* 2005; 288: R1063–R1070.
6. Dixon JB, Bhathal PS and O'Brien PE. Nonalcoholic fatty liver disease: predictors of nonalcoholic steatohepatitis and liver fibrosis in the severely obese. *Gastroenterology* 2001; 121: 91–100.
7. Leandro G, Mangia A, Hui J, et al. Relationship between steatosis, inflammation, and fibrosis in chronic hepatitis C: a meta-analysis of individual patient data. *Gastroenterology* 2006; 130: 1636–1642.
8. Pais R, Pascale A, Fedchuck L, Charlotte F, Poynard T and Ratziu V. Progression from isolated steatosis to steatohepatitis and fibrosis in nonalcoholic fatty liver disease. *Gastroenterol Clin Biol* 2010: in press.
9. Yoshiji H, Noguchi R, Ikenaka Y, et al. Losartan, an angiotensin-II type 1 receptor blocker, attenuates the liver fibrosis development of non-alcoholic steatohepatitis in the rat. *BMC Res Notes* 2009; 2: 70.
10. Ueki M, Koda M, Shimizu T, Mitsuta A, Yamamoto T and Murawaki Y. Effect of an angiotensin-II type-1 receptor blocker, candesartan on hepatic fibrosis in chronic hepatitis C: a prospective study. *Hepatogastroenterology* 2009; 56: 1100–1104.
11. Yamaguchi K, Yang L, McCall S, et al. Inhibiting triglyceride synthesis improves hepatic steatosis but exacerbates liver damage and fibrosis in obese mice with nonalcoholic steatohepatitis. *Hepatology* 2007; 45: 1366–1374.
12. Saito K, Ishizaka N, Hara M, et al. Lipid accumulation and transforming growth factor-beta upregulation in the kidneys of rats administered angiotensin II. *Hypertension* 2005; 46: 1180–1185.
13. Hongo M, Ishizaka N, Furuta K, et al. Administration of angiotensin II, but not catecholamines, induces accumulation of lipids in the rat heart. *Eur J Pharmacol* 2009; 604: 87–92.
14. Ishizaka N, Matsuzaki G, Saito K, Noiri E, Mori I and Nagai R. Expression and localization of PDGF-B, PDGF-D, and PDGF receptor in the kidney of angiotensin II-infused rat. *Lab Invest* 2006; 86: 1285–1292.
15. Ishizaka N, de Leon H, Laursen JB, et al. Angiotensin II-induced hypertension increases heme oxygenase-1 expression in rat aorta. *Circulation* 1997; 96: 1923–1929.
16. Ishizaka N, Aizawa T, Yamazaki I, et al. Abnormal iron deposition in renal cells in the rat with chronic angiotensin II administration. *Lab Invest* 2002; 82: 87–96.
17. Aizawa T, Ishizaka N, Taguchi J, et al. Heme oxygenase-1 is upregulated in the kidney of angiotensin II-induced hypertensive rats: possible role in renoprotection. *Hypertension* 2000; 35: 800–806.
18. Hongo M, Ishizaka N, Furuta K, et al. Administration of angiotensin II, but not catecholamines, induces accumulation of lipids in the rat heart. *Eur J Pharmacol* 2008; 604: 87–92.
19. Ohno T, Horio F, Tanaka S, Terada M, Namikawa T and Kitoh J. Fatty liver and hyperlipidemia in IDDM (insulin-dependent diabetes mellitus) of streptozotocin-treated shrews. *Life Sci* 2000; 66: 125–131.
20. Sun L, Halaihel N, Zhang W, Rogers T and Levi M. Role of sterol regulatory element-binding protein 1 in regulation of renal lipid metabolism and glomerulosclerosis in diabetes mellitus. *J Biol Chem* 2002; 277: 18919–18927.
21. Ueno M, Suzuki J, Zenimaru Y, et al. Cardiac overexpression of hormone-sensitive lipase inhibits myocardial

steatosis and fibrosis in streptozotocin diabetic mice. *Am J Physiol Endocrinol Metab* 2008; 294: E1109–E1118.
22. Yu BC, Chang CK, Ou HY, Cheng KC and Cheng JT. Decrease of peroxisome proliferator-activated receptor delta expression in cardiomyopathy of streptozotocin-induced diabetic rats. *Cardiovasc Res* 2008; 80: 78–87.
23. Matsuzaka T, Shimano H, Yahagi N, et al. Insulin-independent induction of sterol regulatory element-binding protein-1c expression in the livers of streptozotocin-treated mice. *Diabetes* 2004; 53: 560–569.
24. Ishizaka N, Hongo M, Matsuzaki G, et al. Effects of the AT(1) receptor blocker losartan and the calcium channel blocker benidipine on the accumulation of lipids in the kidney of a rat model of metabolic syndrome. *Hypertens Res* 2010; 33: 263–268.
25. Viollet B, Foretz M, Guigas B, et al. Activation of AMP-activated protein kinase in the liver: a new strategy for the management of metabolic hepatic disorders. *J Physiol* 2006; 574: 41–53.
26. Yang J, Maika S, Craddock L, King JA and Liu ZM. Chronic activation of AMP-activated protein kinase-alpha1 in liver leads to decreased adiposity in mice. *Biochem Biophys Res Commun* 2008; 370: 248–253.
27. Hagstrom-Toft E, Thorne A, Reynisdottir S, et al. Evidence for a major role of skeletal muscle lipolysis in the regulation of lipid oxidation during caloric restriction in vivo. *Diabetes* 2001; 50: 1604–1611.
28. van der Meer RW, Hammer S, Smit JW, et al. Short-term caloric restriction induces accumulation of myocardial triglycerides and decreases left ventricular diastolic function in healthy subjects. *Diabetes* 2007; 56: 2849–2853.
29. Hammer S, van der Meer RW, Lamb HJ, et al. Progressive caloric restriction induces dose-dependent changes in myocardial triglyceride content and diastolic function in healthy men. *J Clin Endocrinol Metab* 2008; 93: 497–503.
30. Brink M, Wellen J and Delafontaine P. Angiotensin II causes weight loss and decreases circulating insulin-like growth factor I in rats through a pressor-independent mechanism. *J Clin Invest* 1996; 97: 2509–2516.
31. Brink M, Price SR, Chrast J, et al. Angiotensin II induces skeletal muscle wasting through enhanced protein degradation and down-regulates autocrine insulin-like growth factor I. *Endocrinology* 2001; 142: 1489–1496.
32. Song YH, Li Y, Du J, Mitch WE, Rosenthal N and Delafontaine P. Muscle-specific expression of IGF-1 blocks angiotensin II-induced skeletal muscle wasting. *J Clin Invest* 2005; 115: 451–458.
33. Cabassi A, Coghi P, Govoni P, et al. Sympathetic modulation by carvedilol and losartan reduces angiotensin II-mediated lipolysis in subcutaneous and visceral fat. *J Clin Endocrinol Metab* 2005; 90: 2888–2897.
34. Kather H, Wieland E, Fischer B, Wirth A and Schlierf G. Adrenergic regulation of lipolysis in abdominal adipocytes of obese subjects during caloric restriction: reversal of catecholamine action caused by relief of endogenous inhibition. *Eur J Clin Invest* 1985; 15: 30–37.
35. Du J, Peng T, Scheidegger KJ and Delafontaine P. Angiotensin II activation of insulin-like growth factor 1 receptor transcription is mediated by a tyrosine kinase-dependent redox-sensitive mechanism. *Arterioscler Thromb Vasc Biol* 1999; 19: 2119–2126.
36. Ma Y, Zhang L, Peng T, et al. Angiotensin II stimulates transcription of insulin-like growth factor I receptor in vascular smooth muscle cells: role of nuclear factor-kappaB. *Endocrinology* 2006; 147: 1256–1263.
37. Ishizaka N, Alexander RW, Laursen JB, et al. G protein-coupled receptor kinase 5 in cultured vascular smooth muscle cells and rat aorta. Regulation by angiotensin II and hypertension. *J Biol Chem* 1997; 272: 32482–32488.
38. Toblli JE, Munoz MC, Cao G, Mella J, Pereyra L and Mastai R. ACE inhibition and AT1 receptor blockade prevent fatty liver and fibrosis in obese Zucker rats. *Obesity (Silver Spring)* 2008; 16: 770–776.
39. Fujita K, Yoneda M, Wada K, et al. Telmisartan, an angiotensin II type 1 receptor blocker, controls progress of nonalcoholic steatohepatitis in rats. *Dig Dis Sci* 2007; 52: 3455–3464.
40. Yamamoto E, Dong YF, Kataoka K, et al. Olmesartan prevents cardiovascular injury and hepatic steatosis in obesity and diabetes, accompanied by apoptosis signal regulating kinase-1 inhibition. *Hypertension* 2008; 52: 573–580.
41. Ran J, Hirano T and Adachi M. Chronic ANG II infusion increases plasma triglyceride level by stimulating hepatic triglyceride production in rats. *Am J Physiol Endocrinol Metab* 2004; 287: E955–961.
42. Ran J, Hirano T and Adachi M. Angiotensin II infusion increases hepatic triglyceride production via its type 2 receptor in rats. *J Hypertens* 2005; 23: 1525–1530.
43. Wei Y, Clark SE, Morris EM, et al. Angiotensin II-induced non-alcoholic fatty liver disease is mediated by oxidative stress in transgenic TG(mRen2)27(Ren2) rats. *J Hepatol* 2008.
44. Wei Y, Clark SE, Thyfault JP, et al. Oxidative stress-mediated mitochondrial dysfunction contributes to angiotensin II-induced nonalcoholic fatty liver disease in transgenic Ren2 rats. *Am J Pathol* 2009; 174: 1329–1337.
45. Huisamen B, Perel SJ, Friedrich SO, Salie R, Strijdom H and Lochner A. ANG II type I receptor antagonism improved nitric oxide production and enhanced eNOS and PKB/Akt expression in hearts from a rat model of insulin resistance. *Mol Cell Biochem* 2011; 349: 21–31.
46. Ogihara T, Asano T, Ando K, et al. Angiotensin II-induced insulin resistance is associated with enhanced insulin signaling. *Hypertension* 2002; 40: 872–879.

A Case of Localized IgG4-Related Thoracic Periarteritis and Recurrent Nerve Palsy

Masao Takahashi, MD, Takashi Shimizu, MD, Tsukasa Inajima, MD, Yumiko Hosoya, MD, Norifumi Takeda, MD, Nobukazu Ishizaka, MD, Hiroshi Yamashita, MD, Yasunobu Hirata, MD and Ryozo Nagai, MD

Abstract: Periarteritis, including periaortitis, is a systemic disorder characterized by an excessive fibroinflammatory reaction that can result in the compromise of great vessels and periarterial/periaortic structures. Recent studies have suggested that IgG4-related inflammation may play a role in chronic periaortitis. These pathologic conditions might represent a systemic disorder with fibrotic reaction rather than local inflammation. In this report, the authors describe a case of a 31-year-old man with marked periaortic fibrous thickening localized to the aortic arch, which was histologically and serologically proven to be IgG4 related. Positron emission tomography showed increased ^{18}F-fluorodeoxyglucose uptake at this region. Histologic examination revealed infiltration of lymphoplasmacytes and marked fibrosis with numerous IgG4-positive plasma cells. The serum concentration of IgG4 was 263 mg/dL. The size of the periaortic mass and ^{18}F-fluorodeoxyglucose uptake at this region markedly decreased under corticosteroid therapy. This case suggests that IgG4-related periarteritis can also occur as a solitary focus in the cardiovascular system.

Key Indexing Terms: Periarteritis; Periaortitis; IgG4-related sclerosing disease. **[Am J Med Sci 2010;XX(X):1–000.]**

Chronic periarteritis and periaortitis are a part of a spectrum of idiopathic diseases characterized by fibroinflammatory reaction surrounding the arteries and the aorta. Chronic periaortitis includes idiopathic retroperitoneal fibrosis and inflammatory abdominal aortic aneurysm, and it is considered as a systemic disorder caused by the extended involvement of the aorta and raised inflammatory markers.[1] On the other hand, IgG (immunoglobulin G) 4-related sclerosing disease is also known as a systemic disorder of protean manifestations that may involve the pancreas,[2] retroperitoneum,[3] bile duct[4] and salivary glands.[5] It has been recently suggested that IgG4-related sclerosing disease may be linked to chronic periarteritis and that these 2 disorders might overlap, at least in part.[1] We encountered a case of IgG4-related periarteritis at the thoracic aortic arch without evidence of other organ involvement.

CASE REPORT

A 31-year-old Japanese man was admitted to our hospital because of an episode of hoarseness with no previous history of any serious disease. He had not been prescribed any medication. He was a current smoker. On physical examination, blood pressure was 116/70 mm Hg, and other vital signs were within normal range. His left vocal cord was paralyzed because of recurrent laryngeal nerve paralysis. A chest radiograph showed abnormal protrusion of the aortic arch (Figure 1A), and computed tomography (CT) revealed a mass surrounding the aorta at its bifurcation to the subclavian artery (Figure 1B). ^{18}F-fluorodeoxyglucose (^{18}F-FDG) positron emission tomography (PET) showed increased tracer uptake at the aortic arch with no abnormal tracer uptake in other regions (Figure 1C). The following laboratory data were obtained: serum C-reactive protein, 0.62 mg/dL; erythrocyte sedimentation rate, 41 mm/hr; IgG, 1884 mg/dL; IgG4, 263 mg/dL; serum soluble interleukin-2 receptor, 458 U/mL; and absence of detectable antinuclear antibodies. IgG4 subtype accounted for 14.0% of the IgG fraction. CT and magnetic resonance imaging showed no abnormality in the lymph nodes, pancreas or retroperitoneum. Histologic analysis of the thoracoscopic biopsy specimen of the mass at the aortic arch demonstrated diffuse infiltration of lymphoplasmacytes and marked fibrosis, with no significantly atypical cells (Figures 2A and 2B).

Immunostaining for CD3 and CD20 showed that the lymphocytes were polyclonal and included mainly CD20-positive B cells and CD3-positive T cells. The number of CD20-positive B cells was larger than that of CD3-positive T cells (Figures 3A and 3B). In addition, immunostaining for IgG4 revealed many IgG4-positive plasma cells within the lesion (Figure 3C). On the basis of these findings, we made the pathologic diagnosis of IgG4-related periarteritis localized to the aortic arch. IgG4-positive disease frequently accompanies sclerosing pancreatitis. However, magnetic resonance cholangiopancreatography showed that in this patient, the pancreatic duct and bile duct were intact. No finding characteristic of sclerosing pancreatitis was observed. Consequently, we treated him with 40 mg of prednisolone daily for localized IgG4-related periarteritis. Eight weeks later, hoarseness was found to have gradually ameliorated, the chest radiograph and CT scan revealed improvement of the periaortic mass (Figures 4A and 4B), abnormal ^{18}F-FDG uptake of the aorta on PET scanning was reduced (Figure 4C) and all laboratory data were within normal range. We tapered the dose of prednisolone to 5 mg, and no signs of recurrence have been observed during the follow-up examinations (1 year).

DISCUSSION

IgG4-related sclerosing disease was first reported as sclerosing pancreatitis.[2] Since then, patients with histologically proven IgG4-positive plasma cell infiltration and/or markedly elevated serum IgG4 levels are being increasingly diagnosed. These abnormal findings lead to the development of IgG4-related diseases, which may affect different organs or tissues such as the bile duct, the salivary glands and the retroperito-

From the Department of Cardiovascular Medicine (MT, TS, TI, YH, NT, NI, HY, YH, RN), Graduate School of Medicine, The University of Tokyo, Hongo, Bunkyo-ku, Tokyo, Japan; and Division of Cardiology (NI), Department of Internal Medicine III, Osaka Medical College, Daigaku-machi, Takatsuki-shi, Osaka, Japan.

Submitted July 30, 2010; accepted in revised form September 9, 2010.

Correspondence: Masao Takahashi, MD, PhD, Department of Cardiovascular Medicine, Graduate School of Medicine, The University of Tokyo, Hongo 7-3-1, Bunkyo-ku, Tokyo 113-8655, Japan (E-mail: masaotakahashi-gi@umin.ac.jp).

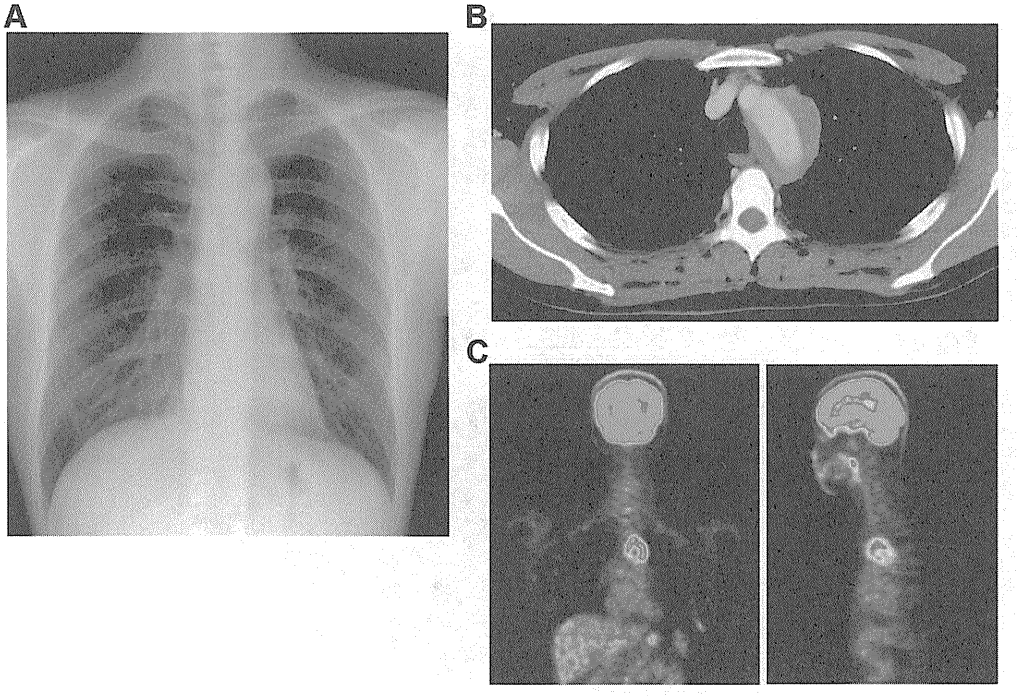

FIGURE 1. Before the corticosteroid therapy, the chest radiograph (A) showed an abnormal protrusion of the aortic arch, contrast medium-enhanced CT (B) of the chest revealed a periaortic mass in the mediastinum and ^{18}F-FDG-PET (C) showed increased tracer uptake at the aortic arch.

neum. Chronic periaortitis is characterized as a fibroinflammatory reaction usually affecting the abdominal aorta. Although the clinical spectrum of chronic periarteritis or periaortitis has not been well defined, retroperitoneal fibrosis and inflammatory abdominal aortic aneurysm are considered to belong to this entity.[1] Of note, there is an increasing body of evidence showing that chronic periaortitis is a feature of IgG4-related sclerosing diseases. For example, in retroperitoneal fibrosis, thickened fibrotic tissue is characterized by diffuse infiltration of IgG4-positive plasma cells.[6] Moreover, IgG4-related diseases can occur not only in tissues near the aorta but also in the wall of arteries including coronary arteries.[7] Therefore, periarteritis is an entity similar to periaortitis.

Although in most cases, the abdominal aorta and neighboring structures are affected, in few cases, only the thoracic aorta is involved.[8,9] One of the reported cases showed not only fibrosis of the thoracic aorta but also retroperitoneal fibrosis with raised IgG4 levels and involvement of other organs.[8] Another patient had an IgG4-related inflammatory aneurysm of the aortic arch whose maximum diameter was 55 mm.[9] In contrast to these 2 cases, no evidence of other organ involvement or of aneurysmal change of the aorta was found in our patient.

It has been suggested that chronic periarteritis and IgG4-related sclerosing disease might represent a systemic inflammatory disorder rather than local inflammatory disease, because each is characterized by constitutional symptoms and raised inflammatory markers with extended involvement of the aorta.[10] However, in our patient, the inflammatory reaction was restricted to the surrounding tissue of the aortic arch, and no abnormal involvement of other organs was detected. The mechanism of solitary and localized involvement in our patient remains to be identified. Some investigators have suggested that local inflammatory reaction to oxidized low-density lipoproteins and ceroids in the atherosclerotic plaques might cause periarteritis.[11] Our patient was a young man with few risk factors for atherosclerosis except for smoking. No atherosclerotic plaque was found in the biopsy specimen.

A recent study reported that T-helper 2 (T_H2) cells and regulatory immune reactions are upregulated in tissues affected by

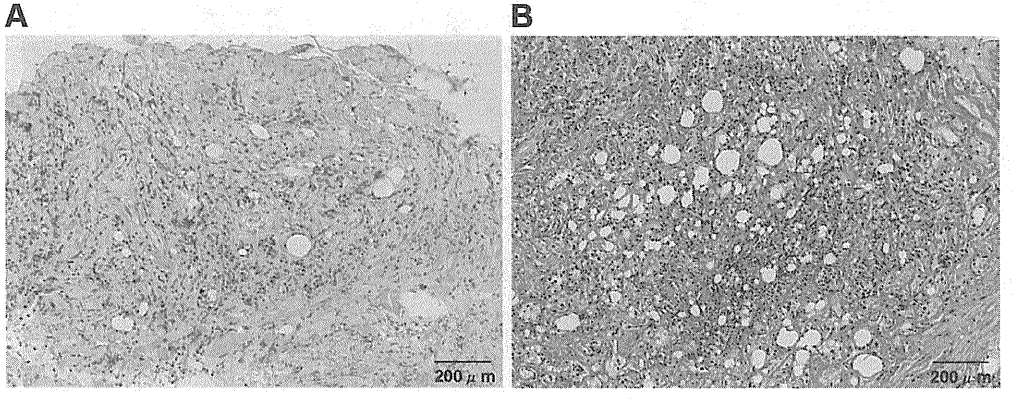

FIGURE 2. Histopathologic findings of the periaortic mass biopsy specimen. Hematoxylin and eosin staining showed lymphoplasmacytic infiltration intermixed with irregular fibrosis (A). Elastic van Gieson stain revealed marked fibrosis (B).

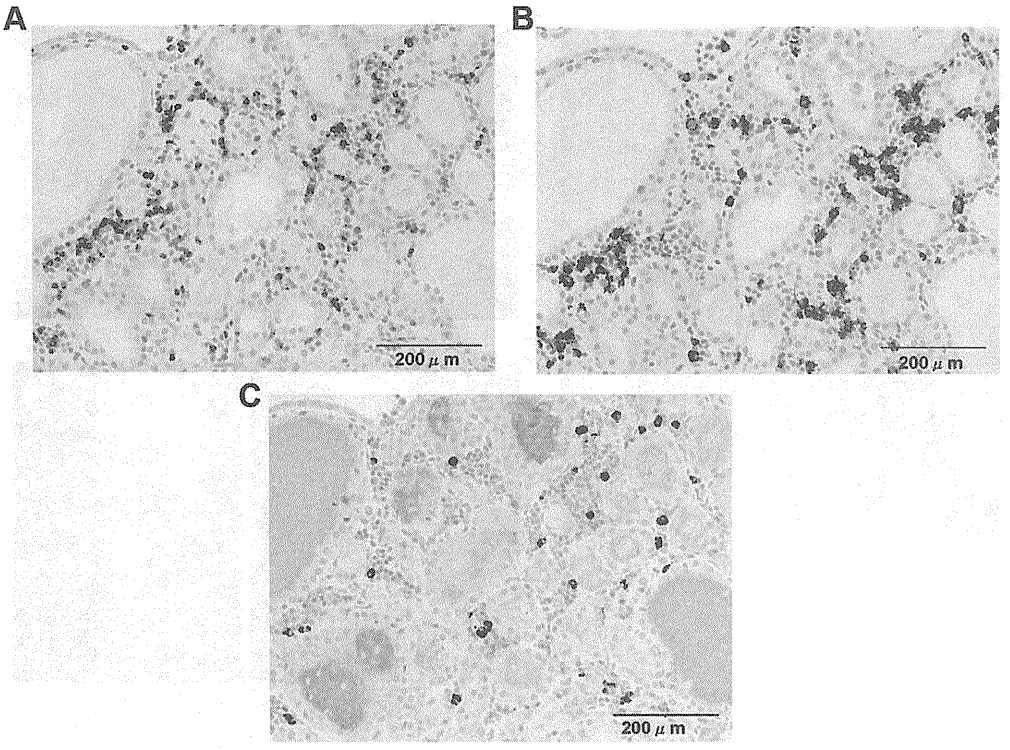

FIGURE 3. Immunostaining of the biopsy specimen for CD3 (A) and CD20 (B) showed that the infiltrate included mainly CD20-positive B cells and CD3-positive T cells. Immunostaining for IgG4 revealed many IgG4-positive plasma cells within the lesion (C).

IgG4-related sclerosing disease,[12] suggesting the involvement of T_H2 cell-mediated immune reaction in the pathogenesis of this disorder. Nevertheless, we did not evaluate the activity of T_H2-associated cytokines before corticosteroid therapy in our patient.

CT revealed a periaortic mass surrounding the aortic arch at a narrow region, and ^{18}F-FDG-PET disclosed remarkably localized tracer uptake. According to these findings, other diseases such as malignant lymphoma should be ruled out. Soluble interleukin-2 receptor level was found to be within normal range (458 U/mL), and serum IgG4 was elevated (263 mg/dL). Although these findings may not be characteristic of a malignant tumor,[6] pathologic examination was considered cru-

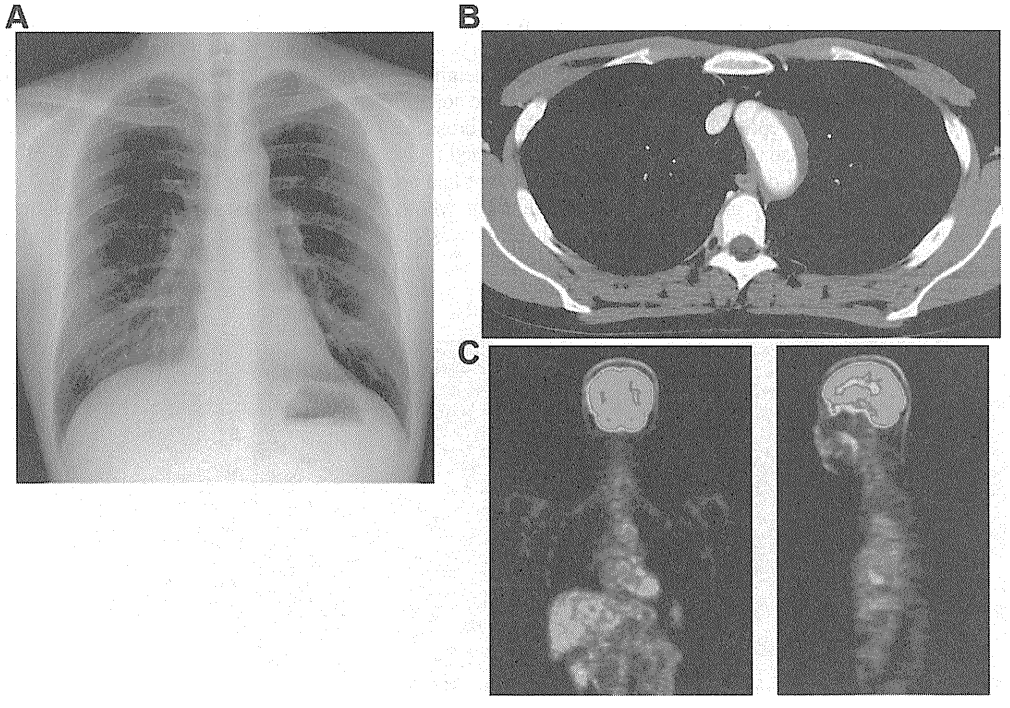

FIGURE 4. After the corticosteroid therapy, the chest radiograph (A) and CT scan (B) revealed a decrease in size of the periaortic mass. PET scanning (C) revealed no abnormal uptake of ^{18}F-FDG at the aortic arch.

cial for the differential diagnosis. Presence of the diffuse infiltration of the IgG4-positive lymphoplasmacytic cells without the evidence of atypicality was useful in distinguishing IgG4-related periarteritis from malignant lymphoma in our case. Serum IgG4 is useful for the diagnosis and evaluation of IgG4-related periarteritis. ^{18}F-FDG-PET is not specific for the diagnosis of IgG4-related periarteritis or chronic periaortitis,[13] but it is useful to assess the progression of the disease and search for other abnormalities in the whole body.

In conclusion, we have presented a case with IgG4-related periarteritis localized to the thoracic aorta. After the induction of corticosteroid therapy, the size of the fibrous mass surrounding the aortic arch decreased, the enhanced uptake of ^{18}F-FDG also decreased and recurrent nerve palsy disappeared. In this patient, accurate diagnosis led to suitable treatment.

REFERENCES

1. **Palmisano A, Vaglio A.** Chronic periaortitis: a fibro-inflammatory disorder. Best Pract Res Clin Rheumatol 2009;23:339–53.
2. **Hamano H, Kawa S, Horiuchi A, et al.** High serum IgG4 concentrations in patients with sclerosing pancreatitis. N Engl J Med 2001;344: 732–8.
3. **Hamano H, Kawa S, Ochi Y, et al.** Hydronephrosis associated with retroperitoneal fibrosis and sclerosing pancreatitis. Lancet 2002;359: 1403–4.
4. **Hamano H, Kawa S, Uehara T, et al.** Immunoglobulin G4-related lymphoplasmacytic sclerosing cholangitis that mimics infiltrating hilar cholangiocarcinoma: part of a spectrum of autoimmune pancreatitis? Gastrointest Endosc 2005;62:152–7.
5. **Kitagawa S, Zen Y, Harada K, et al.** Abundant IgG4-positive plasma cell infiltration characterizes chronic sclerosing sialadenitis (Kuttner's tumor). Am J Surg Pathol 2005;29:783–91.
6. **Zen Y, Onodera M, Inoue D, et al.** Retroperitoneal fibrosis: a clinicopathologic study with respect to immunoglobulin G4. Am J Surg Pathol 2009;33:1833–9.
7. **Matsumoto Y, Kasashima S, Kawashima A, et al.** A case of multiple immunoglobulin G4-related periarteritis: a tumorous lesion of the coronary artery and abdominal aortic aneurysm. Hum Pathol 2008;39: 975–80.
8. **Zen Y, Sawazaki A, Miyayama S, et al.** A case of retroperitoneal and mediastinal fibrosis exhibiting elevated levels of IgG4 in the absence of sclerosing pancreatitis (autoimmune pancreatitis). Hum Pathol 2006; 37:239–43.
9. **Ishida M, Hotta M, Kushima R, et al.** IgG4-related inflammatory aneurysm of the aortic arch. Pathol Int 2009;59:269–73.
10. **Vaglio A, Corradi D, Manenti L, et al.** Evidence of autoimmunity in chronic periaortitis: a prospective study. Am J Med 2003;114:454–62.
11. **Vaglio A, Salvarani C, Buzio C.** Retroperitoneal fibrosis. Lancet 2006;367:241–51.
12. **Zen Y, Fujii T, Harada K, et al.** Th2 and regulatory immune reactions are increased in immunoglobin G4-related sclerosing pancreatitis and cholangitis. Hepatology 2007;45:1538–46.
13. **Pipitone N, Ghinoi A, Versari A, et al.** Images in cardiovascular medicine. Chronic periaortitis. Circulation 2008;118:1214–6.

Novel Insights from Clinical Experience

CARDIOLOGY

Cardiology 2011;120:22–26
DOI: 10.1159/000332996

Received: August 22, 2011
Accepted: August 23, 2011
Published online: November 16, 2011

Giant Tumorous Legions Surrounding the Right Coronary Artery Associated with Immunoglobulin-G4-Related Systemic Disease

Masayasu Ikutomi[a] Takayoshi Matsumura[a] Hiroshi Iwata[a] Go Nishimura[a]
Nobukazu Ishizaka[a] Yasunobu Hirata[a] Minoru Ono[b] Ryozo Nagai[a]

Departments of [a]Cardiovascular Medicine and [b]Cardiothoracic Surgery, The University of Tokyo, Tokyo, Japan

Established Facts

- A novel clinicopathological entity, immunoglobulin-G4-related systemic disease, can affect a wide variety of organs including the pancreas, bile duct, salivary glands and retroperitoneum.
- Further, immunoglobulin-G4-related systemic disease can be manifested as periarteritis, often as inflammatory abdominal aortic aneurysm.

Novel Insights

- Immunoglobulin-G4-related periarteritis can involve the coronary arteries.
- Immunoglobulin-G4-related systemic disease should be considered in any patient with abnormally increased wall thickness or ectatic lesions in the coronary arteries.

Key Words
Immunoglobulin-G4-related systemic disease · Coronary periarteritis · Autoimmune disease

Abstract
Immunoglobulin G4 (IgG4)-related systemic disease was first recognized as a clinicopathological entity about 10 years ago, and since then, it has attracted growing attention. It is an autoimmune disease which affects multiple organs including the pancreas, bile duct, salivary glands and retroperitoneum. Further, it was recently reported that it can be manifested as periarteritis, often as inflammatory abdominal aortic aneurysm. We describe the case of a 75-year-old man with autoimmune pancreatitis and parotitis who presented with angina. The serum concentration of IgG4 was significantly increased at 2,510 mg/dl. Coronary angiography showed multiple stenotic lesions and pronounced dilatation of the right coronary artery. Cardiac computed tomography disclosed increased wall thickness of the coronary arteries and focal tumorous lesions surrounding the right coronary artery. Treatment with steroids proved only marginally effective and he underwent surgical resection of the aneurysm and coronary artery bypass grafting. The diag-

KARGER

Fax +41 61 306 12 34
E-Mail karger@karger.ch
www.karger.com

0008–6312/11/1201–0022$38.00/0

Accessible online at:
www.karger.com/crd

Takayoshi Matsumura
Department of Cardiovascular Medicine
The University of Tokyo, 7-3-1 Hongo, Bunkyo-ku
Tokyo 113-8655 (Japan)
Tel. +81 3 3815 5411, ext. 33117, E-Mail tamatsum-tky@umin.ac.jp

nosis of IgG4-related systemic disease was confirmed by histological examination of the resected mass, which showed a massive infiltration of IgG4-positive plasma cells. This case emphasizes the importance of considering the diagnosis in any patient with abnormally increased wall thickness or ectatic lesions in the coronary arteries.

Introduction

Immunoglobulin G4 (IgG4)-related systemic disease is an autoimmune disorder in which IgG4-positive plasma cells infiltrate and expand in affected organs [1–6]. It was first recognized to involve the pancreas and is now known to involve diverse organs including not only the pancreas but also the bile duct, salivary glands, kidneys, lungs, retroperitoneum and aorta [7–10]. The spectrum of IgG4-related systemic disease is growing steadily, and it can be underdiagnosed simply due to a lack of awareness of this condition. We present a patient with IgG4-related coronary periarteritis in whom tumorous lesions surrounding the coronary arteries were demonstrated by cardiac computed tomography.

Case Report

A 75-year-old man was referred to our department for chest pain on exertion. He had a long history of diabetes mellitus, hyperlipidemia and hypertension, which had been adequately controlled with medications. At the age of 70 years, autoimmune pancreatitis was diagnosed by elevated serum IgG4 concentration and the findings on abdominal computed tomography and magnetic resonance imaging. It had been followed up without steroid therapy due to the lack of clinical symptoms. Also recently, he had bilateral parotitis with painful swelling of the parotid glands. On admission, he had severe xanthomas of the Achilles tendons and on the dorsum of the hands. Thus, a possible diagnosis of familial hypercholesterolemia was made, which was further supported by his family history of early atherosclerotic disease. Laboratory data showed an increase in erythrocyte sedimentation rate (112 mm/h). In addition, the serum concentration of total IgG was increased substantially (3,566 mg/dl, normal range 800–1,600), and the serum IgG4 level was dramatically elevated at 2,510 mg/dl (normal range 4.8–105).

Coronary angiography showed diffuse severe stenosis of the left anterior descending artery and focal stenosis in the proximal left circumflex artery (fig. 1a), and the right coronary artery was generally ectatic with pronounced dilatation of the distal segment (fig. 1b). Cardiac computed tomography disclosed increased wall thickness of the coronary arteries and, of note, two focal tumorous lesions surrounding the middle and distal portion of the right coronary artery were revealed (fig. 2a). The wall thickness of the aortic arch and the abdominal aorta was also increased (fig. 3). ^{18}F-fluorodeoxyglucose positron-emission tomography demonstrated intense uptake not only in the pancreas and the parotid glands, but also in the wall of the coronary arteries, suggesting active inflammation in these lesions (fig. 4).

The patient was clinically diagnosed with IgG4-related systemic disease and treated with prednisone 30 mg daily, followed by a taper of the daily dose by 5 mg per 2-week period. The swelling of the parotid glands resolved soon. The serum levels of total IgG and IgG4 decreased significantly to 1,266 and 676 mg/dl, respectively, and the diffuse pancreatic mass was reduced in size in 4 weeks. On the other hand, the thickened walls and tumorous tissues around the coronary arteries and the ectatic lesion of the right coronary artery were only marginally improved. The stenosis of the left cor-

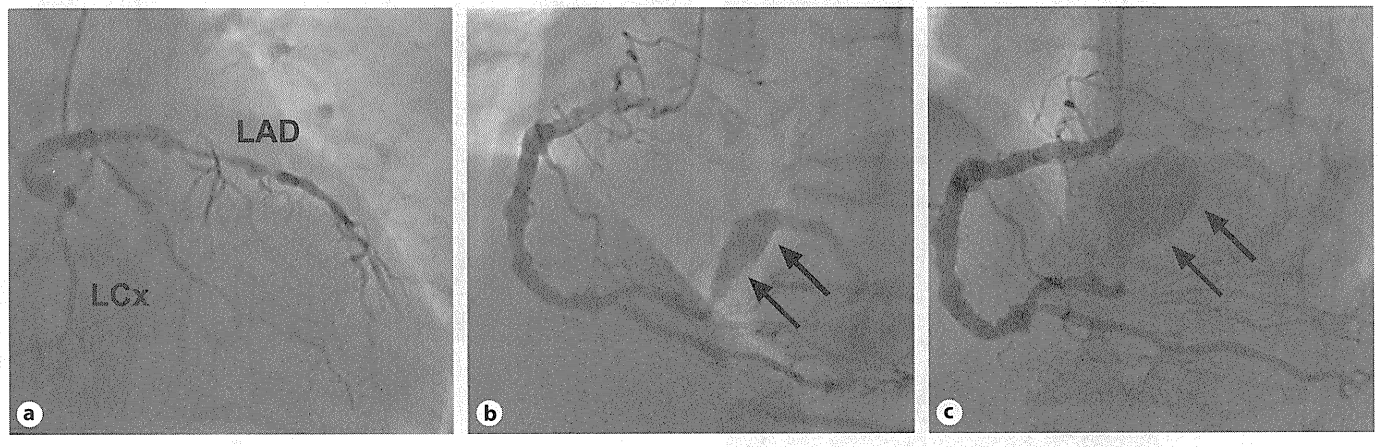

Fig. 1. Coronary angiography on first admission (**a**, **b**) and 4 months later (**c**). **a** Coronary angiography on first admission showing diffuse severe stenosis of the left anterior descending artery (LAD) and focal stenosis in the proximal left circumflex artery (LCx). **b** The right coronary artery was generally ectatic with pronounced dilatation of the distal segment (arrows). **c** Four months later, the ectatic lesion of the right coronary artery was further dilated (arrows).

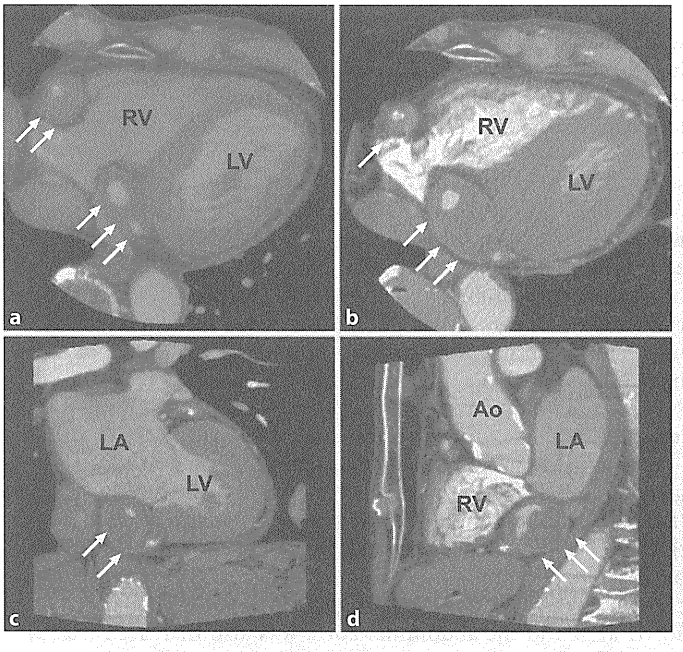

Fig. 2. Cardiac computed tomography on first admission (**a**) and 4 months later (**b–d**). RV = Right ventricle; LV = left ventricle; LA = left atrium; Ao = aorta. **a** Horizontal view of cardiac computed tomography on first admission demonstrating focal tumorous lesions surrounding the right coronary artery (arrows). **b–d** Four months later, the tumorous tissue in the distal portion (arrows) enlarged, as shown by horizontal (**b**), coronal (**c**) and sagittal view (**d**).

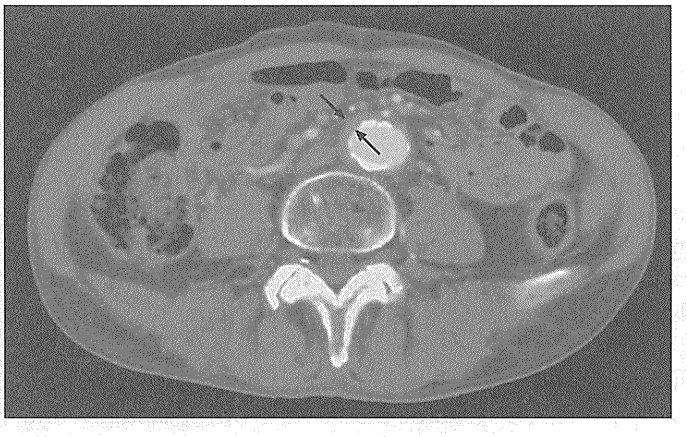

Fig. 3. Abdominal computed tomography showing the increased wall thickness of the abdominal aorta (arrows).

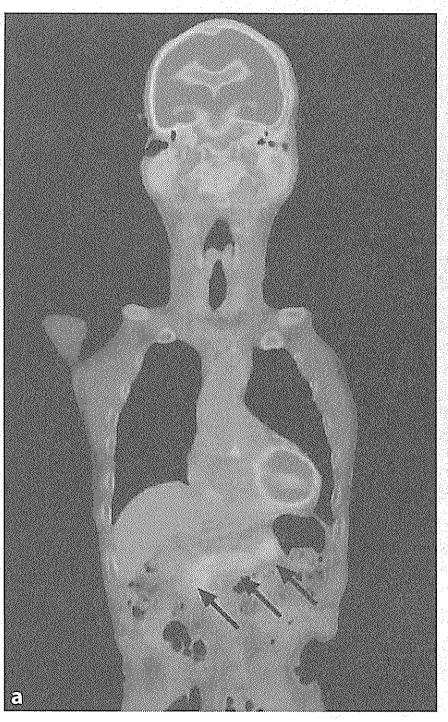

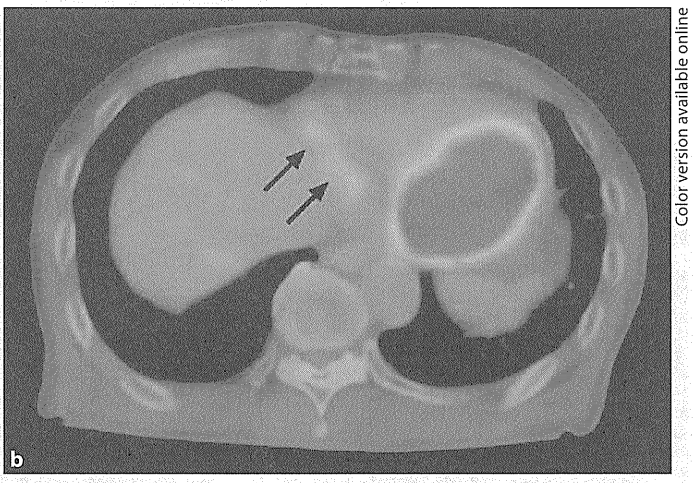

Color version available online

Fig. 4. ^{18}F-fluorodeoxyglucose positron-emission tomography demonstrating intense uptake not only in the pancreas (arrows) and the parotid glands (**a**), but also in the wall of the coronary arteries (arrows, **b**).